

Phase diagram of $d = 4$ Ising Model with two couplings

J. L. Alonso^a, J. M. Carmona^a,
J. Clemente Gallardo^a, L. A. Fernández^b,
D. Iñiguez^a, A. Tarancón^a, C. L. Ullod^a

November 30, 2021

a) Departamento de Física Teórica, Facultad de Ciencias,
Universidad de Zaragoza, 50009 Zaragoza, Spain

b) Departamento de Física Teórica I, Facultad de Ciencias Físicas,
Universidad Complutense de Madrid, 28040 Madrid, Spain

Abstract

We study the phase diagram of the four dimensional Ising model with first and second neighbour couplings, specially in the antiferromagnetic region, by using Mean Field and Monte Carlo methods. From the later, all the transition lines seem to be first order except that between ferromagnetic and disordered phases in a region including the first-neighbour Ising transition point.

Antiferromagnetism has been considered in a great variety of models in order to find properties not present in the purely ferromagnetic (FM) system. Mostly they have been models in two and three dimensions. For instance, in several works on High Temperature Superconductivity the transition from paramagnetic (PM) to non-pure FM ordered phases has been studied [1, 2, 3, 4]. On the other hand, in relation to the finite temperature phase transition in pure gauge $SU(3)$, the $d = 3$ three state Potts model with negative second neighbour couplings was unsuccessfully considered to find a new critical behaviour [5, 6].

In four dimensions, in diluted systems recently new critical exponents have been obtained [7]. From a quantum field theory point of view, no argument appears to prevent the existence of a non-trivial ultraviolet limit in an antiferromagnetic (AF) lattice ϕ^4 theory [8]. In fact, Gallavotti and Rivasseau more than ten years ago considered the possibility of an AF action which could change the ultraviolet limit of the pure ϕ^4 model [9].

Motivated in part by that, we decided to study the phase diagram and possible critical behaviour of a $d = 4$ Ising model with an AF phase non trivially equivalent to the standard FM one. As we will see, we have found a rich phase diagram with several phase transitions but none of them seems to show a new critical behaviour.

The naive way to introduce antiferromagnetism in the Ising model is to consider a negative coupling. In this case the state with minimal energy for large β is a staggered vacuum. On a hypercubic lattice, we denote the coordinates of site \vec{n} as (n_x, n_y, n_z, n_t) . If we make the transformation

$$\sigma(n_x, n_y, n_z, n_t) \rightarrow (-1)^{n_x+n_y+n_z+n_t} \sigma(n_x, n_y, n_z, n_t), \quad (1)$$

the system with negative β is mapped onto the positive β one, both regions being exactly equivalent.

Therefore, to consider true antiferromagnetism we must take into account either different geometries or more couplings, in order to make the transformation (1) not an exact mapping. The option we have chosen here is to add a coupling between points at a distance of $\sqrt{2}$ lattice units.

So, we will work with an Ising model with Hamiltonian

$$H = \beta_1 \sum_{\vec{n}, \mu} \sigma(\vec{n}) \sigma(\vec{n} + \vec{\mu}) + \beta_2 \sum_{\vec{n}, \mu, \pm\nu (\mu < \nu)} \sigma(\vec{n}) \sigma(\vec{n} + \vec{\mu} + \vec{\nu}), \quad (2)$$

on a four dimensional hypercubic lattice, with side L and periodic boundary conditions. Here $\vec{\mu}$ denotes the unitary vector in the μ direction.

The transformation (1) maps the semiplane $\beta_1 > 0$ onto the $\beta_1 < 0$ one, and therefore only the region with $\beta_1 \geq 0$ will be considered. On the line $\beta_1 = 0$ the system decouples into two independent sublattices.

The presence of two couplings with opposite signs makes frustration to appear, and very different vacua are possible. For small values of β_1 and β_2 the system is disordered (PM phase). On the other hand, we have computed the configurations which minimize the energy for several asymptotic values of the parameters. We have

only considered configurations with periodicity two. More complex structures have not been observed in our simulations.

We have found the following regions:

1. Small absolute values of β_1, β_2 . PM phase.
2. Large positive β_1, β_2 , or large $\beta_1 > 0, \beta_2 < 0$ with $\beta_1 > 6|\beta_2|$. The vacuum is the FM one, $\sigma(\vec{n}) = \sigma_0$ (σ_0 stands for a fixed spin).
3. Large $\beta_1 > 0, \beta_2 < 0$ with $\beta_1 < 6|\beta_2|$ and $\beta_1 > 2|\beta_2|$. In this region the vacuum is an FM configuration on a three-dimensional cube and AF on the other direction μ . We have 4 identical possibilities to break the symmetry: one for every possible choice of μ (more precisely 8 if we consider also the global $\sigma(\vec{n}) \rightarrow -\sigma(\vec{n})$ symmetry). We call this vacuum Hyperplane Antiferromagnetic (HPAF). The configuration is of type $\sigma(\vec{n}) = (-1)^{n_\mu} \sigma_0$, where μ can be any direction.
4. Large $\beta_1 > 0, \beta_2 < 0$ with $\beta_1 < 2|\beta_2|$. In this region the vacuum is an FM configuration on a two-dimensional plane and AF on the other two directions. We have now six equivalent vacua. We call this vacuum Plane Antiferromagnetic (PAF), and the configuration can be written as $\sigma(\vec{n}) = (-1)^{n_\mu + n_\nu} \sigma_0$, where μ, ν ($\mu < \nu$) can be any direction.

We remark that, in order to avoid undesirable (frustrating) boundary effects for ordered phases, we work with even lattice side L as periodic boundary conditions are imposed.

Now we must define an order parameter for every phase.

For the FM phase the order parameter is the standard magnetization

$$M_1 = (1/V) \sum_{\vec{n}} \sigma(\vec{n}), \quad (3)$$

where V is the lattice volume.

In the HPAF phase we define the parameter $M_{2,\mu} = (1/V) \sum_{\vec{n}} (-1)^{n_\mu} \sigma(\vec{n})$. $M_{2,\mu}$ will be different from zero only in the HPAF phase, where the system becomes antiferromagnetic on the μ direction. We have 4 order parameters (one for every possible value of μ) and only one of them will be different from zero in the HPAF phase. To consider only one, we define

$$M_2 = \sqrt{\sum_{\mu} M_{2,\mu}^2}, \quad (4)$$

that, although it is not a true order parameter, is more appropriate for measuring on a finite lattice.

For the PAF region we first define $M_{3,\mu,\nu} = (1/V) \sum_{\vec{n}} (-1)^{n_\mu + n_\nu} \sigma(\vec{n})$. The same previous discussion applies, and we will work with

$$M_3 = \sqrt{\sum_{\mu < \nu} M_{3,\mu,\nu}^2}. \quad (5)$$

To understand the behaviour of the system, we have carried out a Mean Field analysis and a Monte Carlo simulation.

From the Mean Field analysis we can plot a general phase diagram. We use the standard technique, also used for gauge theories, [10]. We define three different order parameters V_1, V_2, V_3 , labelling the FM, HPAF and PAF phases respectively.

Our Mean Field ansatz is a combination of the three possible order parameters

$$V(\vec{n}) = V_1 + (-1)^{n_x} V_2 + (-1)^{n_x+n_y} V_3, \quad (6)$$

with their corresponding auxiliary fields $A(\vec{n}) = A_1 + (-1)^{n_x} A_2 + (-1)^{n_x+n_y} A_3$, where we have selected a fixed breaking direction for the HPAF and the PAF phases.

After a standard computation, the free energy per site becomes

$$F = -[(4\beta_1 + 12\beta_2)V_1^2 + 2\beta_1 V_2^2 - 4\beta_2 V_3^2 + A_1 V_1 + A_2 V_2 + A_3 V_3 + T], \quad (7)$$

with T defined as

$$T = (1/4)[\log \cosh(A_1 + A_2 + A_3) + \log \cosh(A_1 + A_2 - A_3) + \log \cosh(A_1 - A_2 + A_3) + \log \cosh(A_1 - A_2 - A_3)]. \quad (8)$$

By solving the saddle point equations for F

$$\frac{\partial F}{\partial V_i} = 0, \quad \frac{\partial F}{\partial A_i} = 0, \quad i = 1, 2, 3, \quad (9)$$

we will find regions in the parameter space where the minimum of F corresponds to different values of V_i .

This system of 6 equations is easily reduced to 3 equations resembling the classical $M = \alpha \tanh(M)$ but they are coupled. By inspection one finds some solutions:

1. $V_1 = V_2 = V_3 = 0$ is always a solution.
2. $V_1 \neq 0, V_2 = V_3 = 0$ is solution if $8\beta_1 + 24\beta_2 > 1$.
3. $V_2 \neq 0, V_1 = V_3 = 0$ if $4\beta_1 > 1$.
4. $V_3 \neq 0, V_1 = V_2 = 0$ if $-8\beta_2 > 1$.

This divides the parameter space in several regions, some of them being mixed. In every region one can see that those are the unique solutions, and the deeper minimum gives the true solution for each pair (β_1, β_2) . The minimum with $V_i = 0 \forall i$ corresponds to the PM phase. If the minimum is at $V_1 \neq 0, V_2 = V_3 = 0$, we are in the FM phase. If only $V_2 \neq 0$, this corresponds to the HPAF phase and, if only $V_3 \neq 0$, the phase is PAF. The result for the phase diagram is shown in Fig. 1.

The transitions separating the different phases are straight lines: $8\beta_1 + 24\beta_2 = 1$ between PM and FM, $4\beta_1 = 1$ for PM-HPAF, $-8\beta_2 = 1$ for PM-PAF, $\beta_1 + 6\beta_2 = 0$

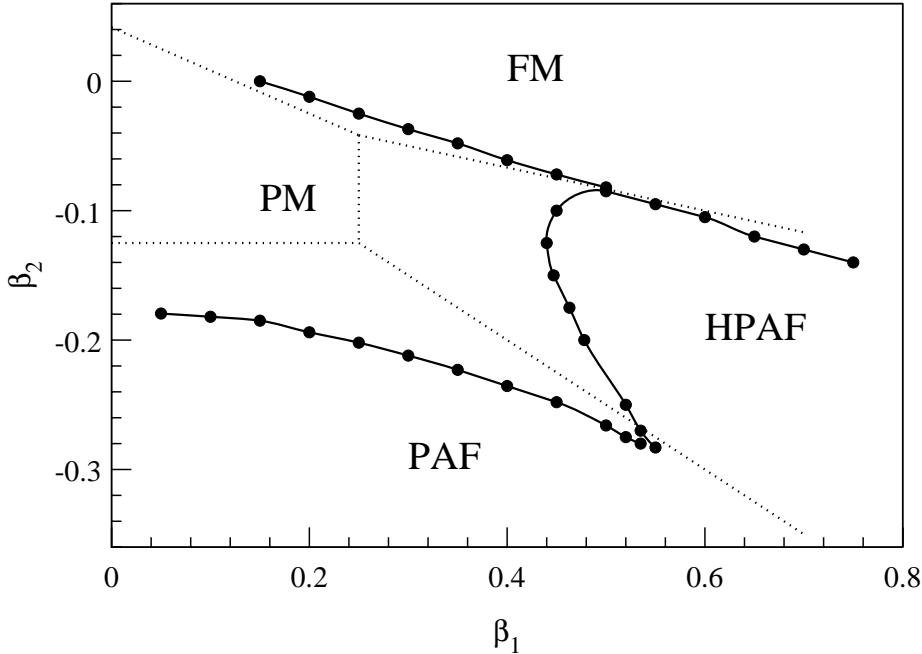


Figure 1: Phase diagram obtained from Mean Field (dotted line) and Monte Carlo (solid line and symbols, the order of the errors is of the size of the symbols).

for FM-HPAF and $\beta_1 + 2\beta_2 = 0$ for PAF-HPAF. The lines between any ordered phase and the PM one are second order with the classical Mean Field exponents (the shape of the equations defining these lines is identical for all of them). The lines between two ordered phases are first order (when crossing the lines an order parameter jumps abruptly from 0 to a positive value).

After this Mean Field approach, we have run a Heat Bath Monte Carlo computation.

We measure the energies, defined as

$$\langle E_1 \rangle = \frac{1}{4V} \frac{\partial \log Z}{\partial \beta_1}, \quad \langle E_2 \rangle = \frac{1}{12V} \frac{\partial \log Z}{\partial \beta_2}, \quad (10)$$

and the expectation value of the order parameters, $\langle M_1 \rangle$, $\langle M_2 \rangle$, $\langle M_3 \rangle$.

With these quantities we have studied the global phase diagram. Using the spectral density method [11] and hysteresis cycles on lattices of size $L = 8$, we have found the transition lines shown in Fig. 1.

The line FM-PM which includes the standard Ising model point ($\beta_2 = 0$) is second order with mean field exponents (from $\beta_1 = 0$ to some β_1 larger than the cited standard critical point).

The transition lines FM-HPAF and HPAF-PAF (see Fig. 1) for large values of β_1 behave as strong first order transitions: they present metastables states and evolve very slowly with our local Monte Carlo simulations. Concerning this, we address the question whether the ordered phases are directly connected or there exists a PM

region between them. We could expect a PM region separating the ordered phases along the asymptotes $\beta_1 + 6\beta_2 = 0$ and $\beta_1 + 2\beta_2 = 0$ (narrower for larger β_1 values) because the ground state is highly degenerate for those values of β_1, β_2 (you can place an FM sublattice beside an HPAF one without the interface increasing the energy, if you choose the correct orientation. You can also do this for the HPAF-PAF case). However, from our MC simulation it is not possible to give a conclusive answer since the width of the hypothetical PM region decreases when increasing β_1 , and for a fixed lattice size there is a practical limit in the precision of the measures of critical values. We have found that the lines PM-FM and PM-HPAF approach very fast and they cannot be resolved for large β_1 values. A similar situation is found when the PM-HPAF line comes near the PM-PAF one. In this case the approaching is even faster.

The transition PM-HPAF presents a clear metastability with a large latent heat, indicating a first order transition.

The transition PM-PAF has a very involved behaviour. For large values of β_1 the transition shows a large latent heat. When we move towards smaller β_1 this latent heat decreases, and for values $\beta_1 \leq 0.20$ it disappears when measured from hysteresis cycles on lattices $L = 8, 12, 16$. This led us to think about the possibility of having a second order transition and study it in a more detailed way.

On this line, we have studied three points: $\beta_1 = 0.1, \beta_1 = 0.05$ and $\beta_1 = 0.0$.

At $\beta_1 = 0.0$ one has two decoupled lattices (one being the constituted by all the first neighbours of the other one). Then we have simulated separately these lattices (we have run on $F4$ lattices). In the following, when we talk about the size of the lattice L at the point $\beta_1 = 0.0$, we will be describing an $F4$ lattice with a number of sites $L^4/2$.

We have simulated lattices from $L = 6$ to $L = 24$. The number of Monte Carlo iterations has depended on the lattice size, going approximately from two hundred thousand (for $L = 6$) to more than one million (for $L = 20, 24$), discarding a quantity of the order of a twenty per cent for thermalization. The largest autocorrelation time found has been $O(10^3)$ for large lattices.

We have used the spectral density method to locate the transition points. No signal of metastability has appeared for the smallest lattices. However on the largest lattices one can observe some trace of a two peak structure. At $\beta_1 = 0.1$ one needs an $L = 20$ lattice to begin to distinguish those signs and at $\beta_1 = 0.05$ one has to go up to $L = 24$. However at $\beta_1 = 0.0$ one can already see a two peak structure at $L = 16$.

In Fig. 2 we show energy histograms at the three points for different lattice sizes.

Besides this direct look at the histograms, we have carried out at those points a Finite Size Scaling analysis [12, 13] using lattices from $L = 6$ to $L = 24$ in order to clarify the order of the transition. Despite one could not strictly talk about critical exponents if the transition resulted to be first order, it is always possible to calculate the exponents with which some quantities diverge with increasing L and see if they agree with those expected for a first order transition ($\nu = 1/d = 0.25, \alpha = 1, \gamma = 1$).

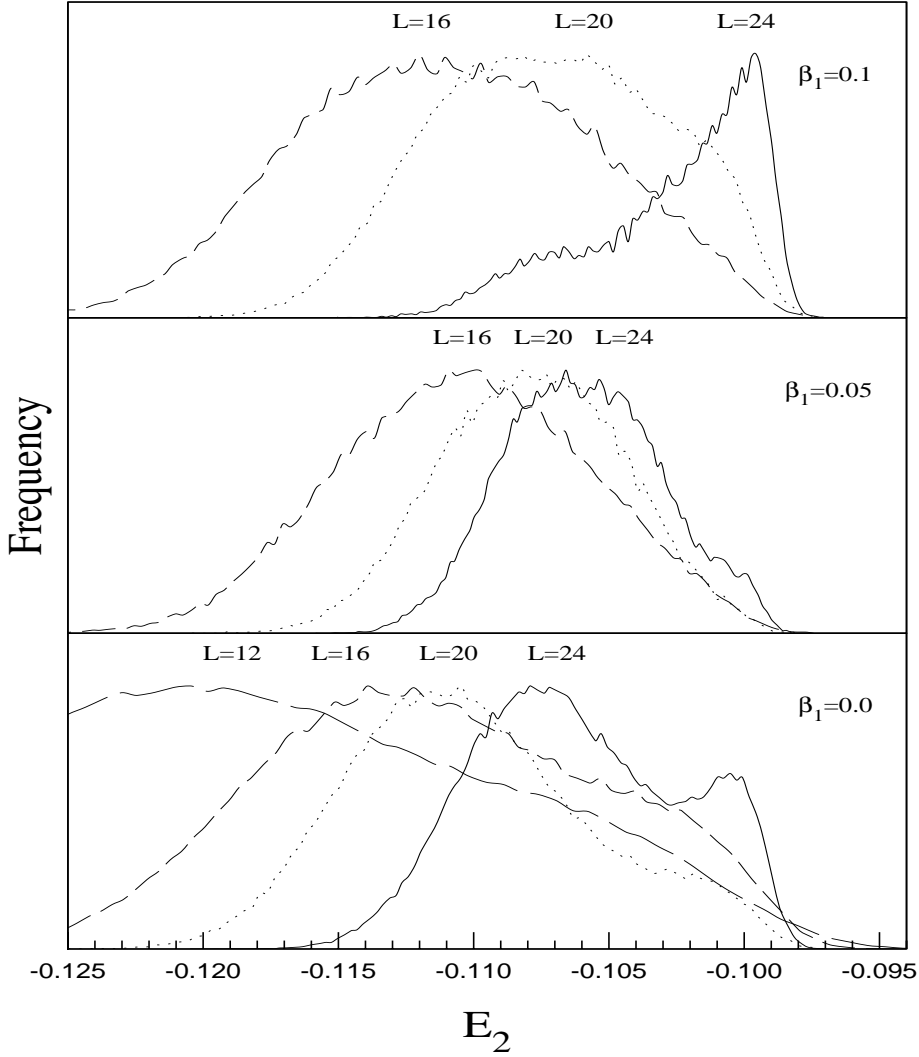


Figure 2: Energy histograms for different lattice sizes in the proximities of the three transition points studied on the line PM-PAF.

We have computed the exponents γ and ν in the way exposed below. A good estimation of α has not been possible. We have used $\langle E_1 \rangle, \langle E_2 \rangle$, the relevant order parameter which is the expectation value of $\langle M_3 \rangle$ ($\langle M \rangle$ hereafter) and some of their derivatives.

We start obtaining ν from the scaling law of the quantity

$$\kappa_i = \frac{\partial \log \langle M \rangle}{\partial \beta_i} = V \left(\frac{\langle M E_i \rangle}{\langle M \rangle} - \langle E_i \rangle \right), \quad (11)$$

which is

$$\kappa_i^{\max}(L) \sim L^{1/\nu}. \quad (12)$$

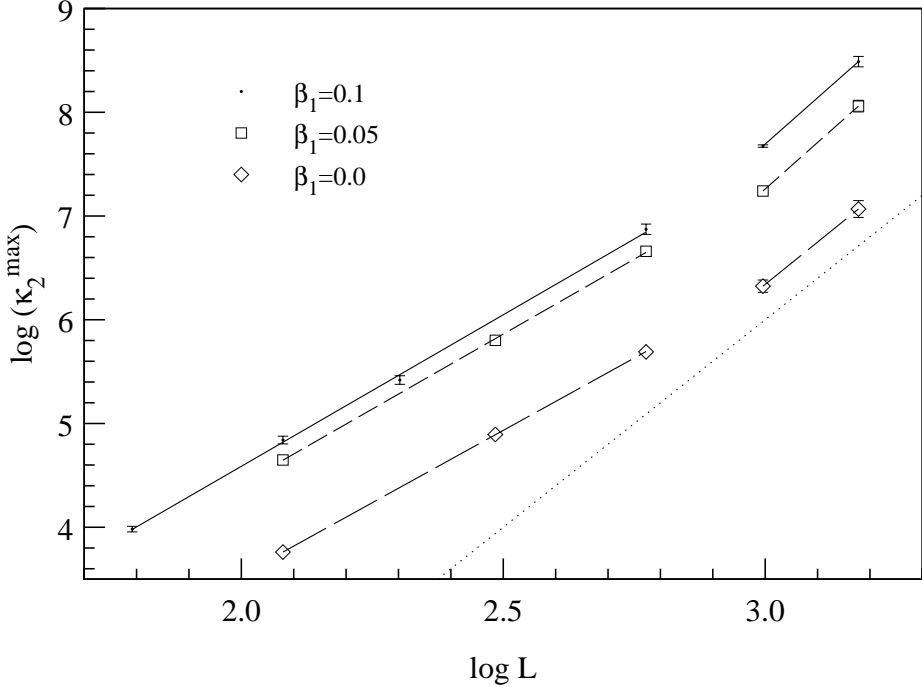


Figure 3: Fits to compute ν from the maxima of κ_2 . The dotted line is for indication (its slope corresponds to $\nu = 1/d$).

To obtain γ we use the susceptibility

$$\chi = V(\langle M^2 \rangle - \langle M \rangle^2), \quad (13)$$

with scaling law

$$\chi_{\max}(L) \sim L^{\gamma/\nu}. \quad (14)$$

The behaviour of the maximal value of κ_2 with L , from where we extract ν , is shown in Fig. 3.

From this figure, it is clear that not all the L values simulated are inside the asymptotic region where one could define a correct ν exponent. Contrarily, one observes that the exponent varies if obtained from different sets of lattice sizes. Notice that the behaviour for $L < 20$ is surprisingly linear, with a slope corresponding to $\nu > 1/d$. However the $L = 20, 24$ lattices point to a value $\nu \simeq 1/d$.

A similar behaviour is found in the computation of γ/ν .

The results for the exponents obtained separately from small and large lattices are shown in Table 1.

On the other hand, we tried to obtain α/ν from the scaling of the elements of the matrix

$$C^{i,j} = \frac{\partial \langle E_i \rangle}{\partial \beta_j}. \quad (15)$$

Its eigenvectors should be respectively orthogonal and parallel to the direction of the transition line. This line is, in this region, almost parallel to the β_1 axis and

		$\beta_1 = 0.0$		$\beta_1 = 0.05$		$\beta_1 = 0.1$	
$d=4$	1 st ord	L=8,12,16	L=20,24	L=8,12,16	L=20,24	L=6,8,10,16	L=20,24
ν	0.25	0.359(4)	0.245(33)	0.346(7)	0.223(16)	0.342(6)	0.224(14)
γ	1	1.08(2)	1.06(23)	1.08(3)	1.03(10)	1.08(3)	1.02(9)

Table 1: Exponents obtained at the three transition points studied on the line PM-PAF using different sets of lattice sizes. The first column refers to the expected for a first order transition.

the $C^{2,2}$ element results to be very close to the eigenvalue corresponding to the orthogonal eigenvector, which will be the only relevant element of the matrix $C^{i,j}$ (it would not be the case if the point were a multicritical point). In short, we studied the divergence of the $C^{2,2}$ matrix element. However we did not get a reasonable estimation of α . There are basically two coupled difficulties. Firstly the divergence of the specific heat is usually difficult to fit. Many times one does not need just a power term in L but also a constant term or even a logarithmic or exponential one. This problem could be solved but the added objection here is that we have very little data inside the asymptotic region, and the estimations we can make for α are too much poor.

A satisfactory conclusion is obtained from the behaviour of the Binder cumulant [14]

$$V = 1 - \frac{\langle E_2^4 \rangle}{3\langle E_2^2 \rangle^2}. \quad (16)$$

The minimum of this observable approaches the value $2/3$ with increasing L in a second order transition. This is not the case if the transition is first order, where in the thermodynamical limit it takes a value depending on the position of the two energy peaks and easily determined from (16). If these peaks are delta functions situated at E_a and E_b , then

$$V_{min} = 1 - \frac{2(E_a^4 + E_b^4)}{3(E_a^2 + E_b^2)^2}. \quad (17)$$

In Fig. 4 it is shown how, despite its closeness to $2/3$, V_{min} tends with increasing L to a value slightly but significantly smaller than this (approximately 0.6658) which indicates a first order transition with a latent heat that can be estimated in the following way. Let write $E_b = E_a + \Delta$. Looking at the histograms (Fig. 2) one observes that, approximately, one peak is situated at an energy of -0.1 and the latent heat Δ is one order of magnitude smaller. Taking that value for E_a and the value 0.6658 for V_{min} in the thermodynamic limit, one obtains from (17) a latent heat $\Delta \simeq -0.005$ which is of the same order as the expected from the histograms.

On the other hand, we have computed the transition points $\beta_2^c(\infty)$ at each β_1 value by using the expression

$$\beta_2^c(\infty) = \beta_2^c(L) - AL^{-1/\nu}. \quad (18)$$

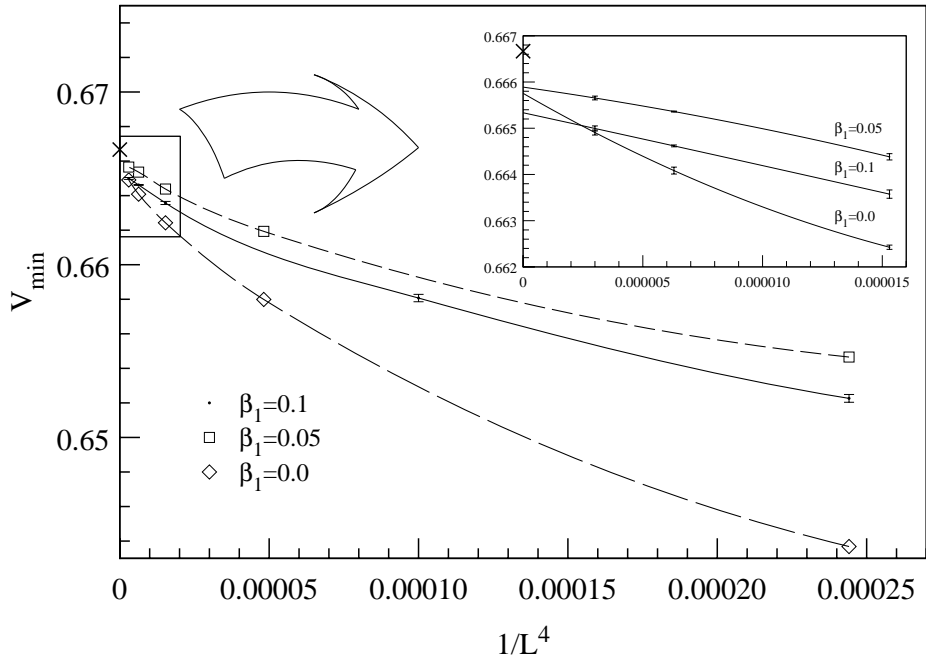


Figure 4: Minimum of the Binder cumulant as a function of the lattice size. The cross marks the value $2/3$.

We have used only the largest values of L and the corresponding exponent ν . For each observable, we have (in principle) a different $\beta_2^c(L)$ obtained as the position of the maximum derivative (with respect to β_2). The resulting $\beta_2^c(\infty)$ is very similar for any of them and we take the mean value. We obtain $\beta_2^c(\infty) = -0.17904(3)$, $-0.17568(8)$, $-0.17459(15)$ at $\beta_1 = 0.1, 0.05, 0.0$ respectively.

As it was met in phase transitions of some other systems with frustration effects and non-trivial sublattice structures, for instance [4, 15], this study has revealed to be hard and we have needed rather large lattices to see the asymptotic behaviour, which was masked up to a significant size ($L = 24$ is a considerably large lattice in $d = 4$). On the other hand, a usual problem in this kind of systems is that they are difficult to equilibrate. However, we have simulated 64 independent lattices starting from different configurations and, after thermalization, they give fully compatible results.

In conclusion, we have described the phase diagram of the four dimensional Ising model with first, β_1 , and second, β_2 , neighbour couplings. In the $\beta_1 > 0$ semiplane, four regions (PM, FM, HPAF and PAF) are present. The $\beta_1 < 0$ semiplane is obtained from the above by means of a trivial transformation. All the transition lines have resulted to be first order except that corresponding to the first neighbour Ising model which is second order with Mean Field exponents. In consequence, this simple modification to the Ising model does not seem, by itself, to be useful for finding a critical behaviour different from the classical one.

Acknowledgments We wish to thank Juan J. Ruiz-Lorenzo for useful discussions, as well as the RTN group for the use of the RTN machine, where part of this work has been done. Partially supported by CICyT AEN93-0604-C03, AEN94-0218, AEN93-0776. D.I., J.C.G. and J.M.C. are MEC Fellows and C.L.U. DGA Fellow.

References

- [1] M.L. Plumer and A. Caillé, *J. Appl. Phys.* **70**(1991)5961.
- [2] H. Kawamura, *J. Phys. Soc. Jpn.* **61**(1992)1299.
- [3] H. Mori and M. Hamada, *Physica B* **194-196**(1994)1445.
- [4] J.L. Morán-López, F. Aguilera-Granja and J.M. Sánchez, *J.Phys.: Cond. Matt.* **6**(1994)9759.
- [5] L.A. Fernández, U. Marini and A. Tarancón, *Phys. Lett.* **B217**(1989)314.
- [6] M. Bernaschi, L. Bifferale, L.A. Fernández, U. Marini, R. Petronzio and A. Tarancón, *Phys. Lett.* **B231**(1989)157.
- [7] G. Parisi and J. J. Ruiz-Lorenzo, *J. of Phys. A: Math. and Gen.* **28**(1995)L395.
- [8] D.J.E. Callaway *Phys. Rep.* **167**(1988)5.
- [9] G. Gallavotti and V. Rivasseau, *Phys. Lett.* **122B**(1983)268.
- [10] J.M Drouffe and J.B. Zuber, *Phys. Rep.* **102C**(1983)74.
- [11] M. Falcioni, E. Marinari, M.L. Paciello, G. Parisi and B. Taglienti, *Phys. Lett.* **108B** (1982)331; A.M. Ferrenberg and R. Swendsen, *Phys. Rev. Lett.* **61** (1988)2635.
- [12] M.E. Fisher and M.N. Barber, *Phys. Rev. Lett.* **28**(1972)1516.
- [13] A. Bunker, B.D. Gaullin and C. Callin, *Phys. Rev.* **B48**(1993)15861.
- [14] M.S.S. Challa, D.P. Landau and K. Binder, *Phys. Rev.* **34**(1986)1841.
- [15] J. Oitmaa and J.F. Fernandez, *Phys. Rev.* **B39**(1989)11920.